Ferromagnetism in metallic chalcospinels $CuCr_2S_4$ and $CuCr_2Se_4$

T. Saha-Dasgupta,[1] Molly De Raychaudhury,[1] and D. D. Sarma[2,3]
[1]*S.N. Bose National Centre for Basic Sciences, Kolkata 700098, India*
[2]*Centre for Advanced Materials, Indian Association for the Cultivation of Science, Jadavpur, Kolkata 700032, India*
[3]*Solid State and Structural Chemistry Unit, Indian Institute of Science, Bangalore 560012, India*

We explore the origin of ferromagnetism in $CuCr_2S_4$ and $CuCr_2Se_4$ by analyzing the computed, *ab initio* electronic structure. Based on our analysis, we establish the kinetic-energy driven mechanism as operative in the case of double perovskites and pyrochlores to be also responsible in these compounds for the experimentally observed ferromagnetism with high Curie temperatures. We provide detailed microscopic understanding of the mechanism in terms of *N*th order muffin-tin orbital based downfolding calculations, estimates of the magnetic exchange coupling, and the ferromagnetic transition temperature, computed in mean-field way.

Spinel-structured compounds have been well known for a long time as an interesting class of materials.[1–4] Among these compounds, Cr-based metallic chalcospinels, $CuCr_2S_4$ and $CuCr_2Se_4$, deserve attention due to the high ferromagnetic (FM) transition temperatures of 377 and 430 K,[5] respectively. The metallic character together with high Curie temperature makes these compounds promising candidates for magneto-optic devices.[6] Soon after the first synthesis of $CuCr_2S_4(Se_4)$ back in 1956 by Hahn *et al.*[7] and the measurement of magnetic properties by Lotgering[8] in 1964, the origin of ferromagnetism has been investigated by many researchers. Lotgering[8] proposed the mixed valent model of Cr^{3+} and Cr^{4+} and invoked the double exchange (DEX) mechanism to explain the simultaneous occurrence of ferromagnetism and metallicity. The subsequent neutron diffraction investigation,[9] however, revealed the presence of only one type of Cr ion, which is in the Cr^{3+} state. They also concluded the presence of a nonlocalized moment of 1 μ_B which is antiparallel to the Cr moment, giving rise to a measured moment of ≈ 5 μ_B instead of 6 μ_B as expected from two Cr^{3+} ions in the unit cell. The above works are based on the assumption of monovalent Cu ions. Goodenough,[10] on the other hand, proposed the Cu ions to be in divalent state with a hole in the Cu *d* manifold, giving rise to metallicity and providing the means of indirect exchange coupling. In recent years, detailed x-ray magnetic circular dichroism (XMCD) study[11] has been carried out to settle this issue. The results conclusively showed that the Cr ion is in the Cr^{3+} state and the tetrahedral sites are occupied by nearly monovalent Cu ions, contrary to Goodenough's proposition.

The origin of ferromagnetism with a high Curie temperature in this class of compounds therefore remained controversial and unresolved. This became particularly interesting with the finding that the nonlocalized moment is antiparallel to the localized Cr moment which does not fit within Hund's coupling driven DEX framework. In the following, we present a detailed analysis of the electronic structure calculations of $CuCr_2S_4(Se_4)$ compounds within the framework of local density approximation (LDA) with an aim to unravel this issue.

The chromium-based spinels $CuCr_2X_4$ (X=S,Se) are normal spinels that crystallize in the face-centered-cubic structure of space group Fd-3m. Cu ions occupy the tetrahedral interstices and Cr ions occupy the octahedral interstices. This results into chains of CrX_6 octahedra linked to CuX_4 tetrahedra which are interconnected to give rise to a three dimensional network. The internal parameter u associated with the anion position controls the $\angle$Cr-X-Cr. The experimentally measured[12] $\angle$Cr-X-Cr turns out to be 94.66° and 93.48° with lattice constants of 9.82 Å and 10.334 Å for X=S and Se, respectively.

In the steps toward unraveling the origin of ferromagnetism, we first note that the presence of a near 90° Cr-X-Cr lattice may locally provide a FM coupling according to Goodenough-Kanamori[13] rule. In order to understand whether such a localized interaction could be primarily responsible for the FM state, we carried out a series of calculations for $CuCr_2S_4$, where we varied the $\angle$Cr-S-Cr over a range of values across the experimentally measured value of 94.66° of the actual compound.[14] We computed the total energy differences associated with the FM configuration of Cr t_{2g} spins parallelly aligned and the antiferromagnetic (AFM) configuration of magnetic Cr sublattice where one of the four nearest neighbor (NN) Cr spins in the tetrahedral unit is put in an antiparallel configuration with respect to the other three. Figure 1 shows the total energy difference plotted as a function of varying $\angle$Cr-S-Cr. The stability of the FM configuration over that of the AFM configuration is found to reduce as the angle tends toward a perfect 90° and increases as the angle increases. The NN exchange couplings J_1, obtained by mapping the LDA total energy differences between FM and AFM spin configurations onto the NN Heisenberg spin Hamiltonian $H=J_1\Sigma_{nn}S_i\cdot S_j$, where S_i denotes the spin-3/2 operator corresponding to the Cr^{+3} spins at the site i, and the mean-field T_c obtained by using $T_c=\frac{S(S+1)}{3k_B}J_1 z$ ($S=\frac{3}{2}$ and the number of NN's z=6), as shown in Table I, support the conclusion that ferromagnetism is destabilized upon decreasing $\angle$Cr-S-Cr toward 90°. This dependence on $\angle$Cr-S-Cr is unexpected since within the Goodenough-Kanamori framework,[13] the interaction between half-filled Cr t_{2g} levels is expected to be more ferromagnetic as $\angle$Cr-S-Cr moves toward 90°. This study, therefore, clearly indicates that the localized interaction is not responsible for the FM state.

In search of the other possible mechanisms, we present in

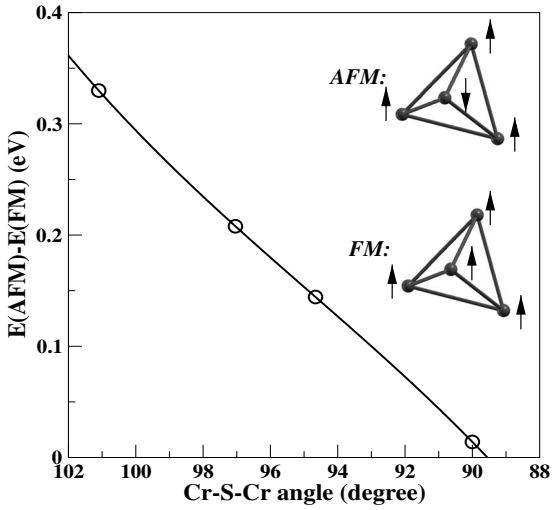

FIG. 1. Total energy difference between AFM and FM spin configurations for a range of ∠Cr-S-Cr, keeping the Cr-S bond length constant in $CuCr_2S_4$. The inset shows the AFM and FM configuration in a Cr tetrahedral unit.

the following the first-principles electronic structure calculations and its analysis. The calculations have been carried out in the tight-binding linear muffin-tin orbital basis.[15,16] The computed spin-polarized electronic structure for $CuCr_2S_4$, shown in Fig. 2, is in agreement with previous published data.[6,11] It exhibits a pseudogaplike feature with low density of states (DOS) of about 1.3 states/eV/f.u. at the Fermi level (E_F) in the minority spin channel, while the majority spin channel is metallic with reasonably high density of states at E_F. The computed net magnetic moment is found to be 5.0 μ_B, in good agreement with experimentally measured value of 4.9 μ_B.[9] The magnetic moment at the Cr site within a muffin-tin (MT) sphere of radius 1.35 Å is found to be 2.7 μ_B, at the Cu site within MT sphere of radius 1.28 Å is −0.08 μ_B, and that at the S site within a MT sphere of radius 1.36 Å is −0.11 μ_B, indicating that the moments associated with S and Cu sites are aligned antiparallel to the moment associated with Cr, in agreement with neutron[9] and XMCD[11] results.[17]

The octahedral surrounding of the Cr atom by the S atoms breaks the degenerate Cr d manifold into Cr t_{2g} and e_g manifolds. The crystal field split Cr e_g states lie about 2 eV above the t_{2g} states and remain empty in both the spin channels. The Cr t_{2g} states, on the other hand, remain almost full in the majority spin channel and almost empty in the minority spin channel in conformity with d^3 or 3+ configuration of the Cr ion. The tetrahedral surrounding of the Cu atom by the S atoms also splits the degenerate Cu d states into t_2 and e

TABLE I. Exchange interaction strength and mean-field T_c calculated within the nearest neighbor model for calculations with ∠Cr-S-Cr=90°, 94.66°, 97°, and 101°.

∠Cr-S-Cr (deg)	101	97	94.66	90
J_1 (meV)	−12.22	−7.7	−5.34	−0.5
T_c (K)	1064	670	465	44

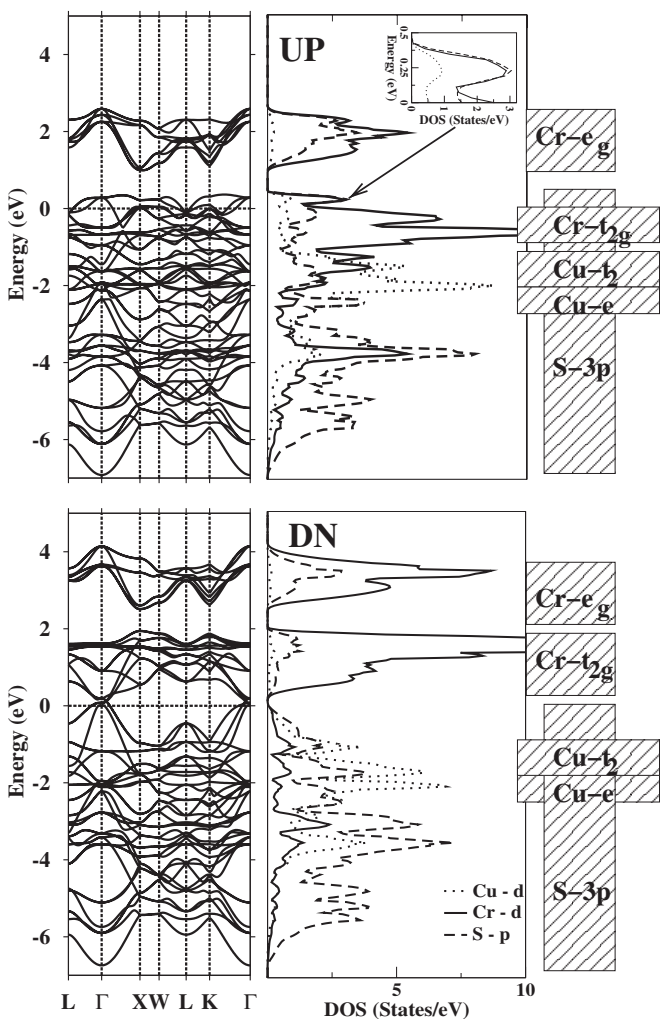

FIG. 2. Left panels show the spin-polarized band structure computed within the local spin density approximation (LSDA) for $CuCr_2S_4$. The zero of the energy is set at the LSDA Fermi energy E_F. Right panels give the spin-polarized density of states. The inset shows the density of states in the majority spin channel in a small energy range close to E_F.

states with t_2 states appearing higher in energy compared to e states as appropriate for a tetrahedrally coordinated cation. The Cu d electrons remain more or less occupied in both the spin channels suggestive of more like the monovalent configuration in agreement with XMCD. The S p states dominate below −2 eV in the occupied bandwidth with significant amount of admixture with Cr d and Cu d states throughout the spectrum shown in Fig. 2.

In the absence of DEX or Goodenough-Kanamori-type superexchange mechanism, a strong candidate in these class of compounds can be the kinetic-energy driven mechanism, similar to that proposed in the case of double perovskites Sr_2FeMoO_6,[18,19] Sr_2FeReO_6, or pyrochlore compounds Tl_2MnO_7.[20] The similarity of the spinels considered here with these compounds is indicated by the fact that $CuCr_2X_4$ too are metallic with high FM transition temperatures and with a delocalized moment aligned antiparallel to the localized moment.[9] The basic electronic structure, described

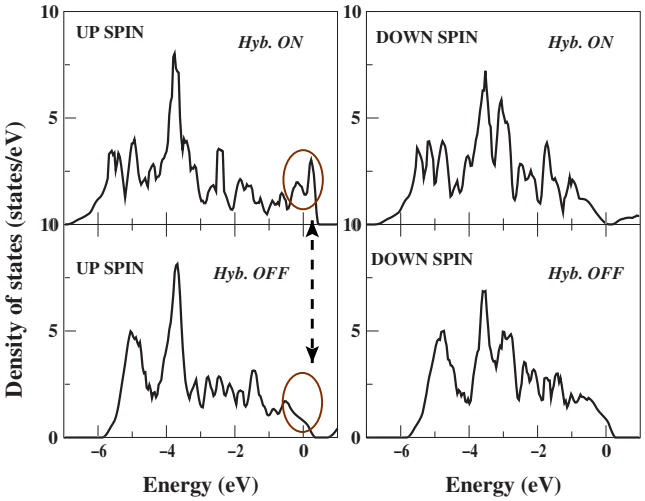

FIG. 3. (Color online) S p density of states of $CuCr_2S_4$ with and without the hybridization between Cr t_{2g} and the S p-Cu d hybrid state.

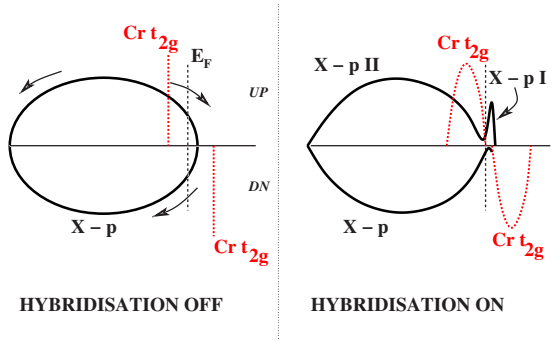

FIG. 4. (Color online) Schematic representation of the exchange mechanism dominant in $CuCr_2X_4$ (X=S, Se).

above, however, shows an apparent contrast with Sr_2FeMoO_6- or $Tl_2Mn_2O_7$-type mechanism. The prerequisite for such a mechanism as explained in Refs. 18 and 19 is the appearance of delocalized levels within the exchange gap of the localized moment which, upon turning on the hybridization between the localized spin and the delocalized levels, give rise to negatively polarized levels with an unoccupied part and a partially occupied part. In the present case, the basic electronic structure does not show this feature. On the other hand, delocalized S p-Cu d states appear generally below the nominally localized Cr d levels, which dominate the top of the occupied part in the majority spin channel and the bottom of the unoccupied part in the minority spin channel.

Nevertheless, interesting things do happen close to E_F in the majority spin channel. The noticeable feature is the small humplike feature just above E_F spanning the energy range of $\approx$0.4 eV separated from the Cr e_g dominated states by a gap of $\approx$0.6 eV, shown as an inset in the right upper panel of Fig. 2. This contains the charge of an extra hole which is primarily responsible for making the material metallic. In order to investigate the origin of this humplike feature, in Fig. 3 we show the S p projected density of states in the presence and in the absence of hybridization between S p-Cu d and Cr t_{2g} states. S p projected DOS contains the mark of the humplike feature in the majority spin channel, which disappears upon turning off the S p-Cu d and Cr t_{2g} hybridization, as highlighted by arrows in the left panel of Fig. 3.

This clearly indicates that the small humplike feature above E_F in the majority spin channel is actually nearly split-off states from the S p-Cu d complex and happens solely due to the hybridization between Cr t_{2g} and S p-Cu d states. We notice that the S p projected DOSs in absence of hybridization looks similar between the majority and minority spin channels, bringing in essentially the nonmagnetic character of S^{2-} ion. Upon turning on the hybridization, they differ from the unhybridized DOS, rather significantly, the effect being more pronounced in the majority spin channel. This hints toward an induced spin splitting at the otherwise nonmagnetic S site, driven entirely by hybridization, thereby restoring back the connection to Sr_2FeMoO_6 or $Tl_2Mn_2O_7$. The situation is schematically shown in Fig. 4. In the absence of the hybridization between the localized Cr t_{2g} levels and the delocalized S p-Cu d band in the minority spin channel, the localized Cr t_{2g} levels appear above the delocalized S p-Cu d band, while in the majority spin channel, the Cr t_{2g} levels appear within the delocalized S p-Cu d complex. Upon switching on the hybridization, the states of the same symmetry and spin couple and the S p-Cu d complex is pushed further down in energy due to hybridization with Cr t_{2g} down spin, while interesting situation happens in the majority spin channel. The portion of the delocalized band appearing below Cr t_{2g} up spin levels is pushed further down, while the part appearing above Cr t_{2g} up spin levels is pushed up, resulting into a large hump (denoted as X-p II in Fig. 4) followed by a dip and a small hump like structure (denoted as X-p I in Fig. 4) close to E_F of the delocalized S p-Cu d band, while the Cr t_{2g} up states appear in the dip. This situation is similar to that in NiAl or NiSi,[21] where ligand p states contribute features close to E_F. As is also obvious from the schematic diagram, this induces a renormalized splitting at the delocalized site which is oppositely oriented to that at the localized Cr site. This, in turn, enforces the parallel alignment of the localized Cr t_{2g} spins.[18–20]

In order to estimate the magnitude of the renormalized spin splitting at the delocalized site, we have employed Nth order muffin-tin orbital (NMTO) *downfolding* technique.[22] This is an energy selective method which provides a few-orbital Hamiltonian starting from a full LDA Hamiltonian by integrating out degrees of freedom that are not of interest. In the present case, we have integrated out all the degrees other than S p to define a few-band S p only Hamiltonian. The on-site energies read from real-space representation of the S p only Hamiltonian show that the on-site splitting between S p I and S p II (see Fig. 4), which is about the same as that between S p I and the down spin S p states, can be as large as 3.9 eV.

Having unraveled the origin of ferromagnetism in $CuCr_2S_4$ and established it to be the same kinetic-energy driven mechanism as operative in the case of double perovskites[18,19] and pyrochlore compounds[20] but manifested in a different manner, we now turn to the sensitive depen-

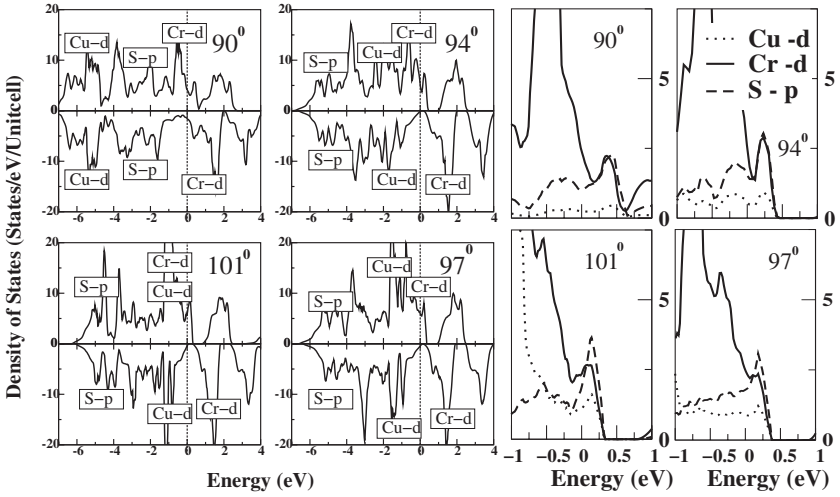

FIG. 5. Left panels: Spin-polarized density of states of Cu d, Cr d, and S p for ∠Cr-S-Cr=90°, 94.66°, 97°, and 101°. The upper (lower) panel shows the majority (minority) spin. Right panels: Zoomed view of the DOS close to E_F in the majority spin channel for ∠Cr-S-Cr =90°, 94.66°, 97°, and 101°.

dence of the FM stability on ∠Cr-S-Cr, discussed right at the beginning. We show in Fig. 5 the DOS calculated with ∠Cr-S-Cr=90°, 94.66°, 97°, and 101°. We notice the relative shifting of the Cu d, Cr t_{2g}, and S p dominated peaks upon varying ∠Cr-S-Cr. Right panels in Fig. 5 show the blown up plot of the density of states, zoomed at the hump region, computed for varying values of ∠Cr-S-Cr. As is clearly seen upon increasing the ∠Cr-S-Cr, the hump region becomes more pronounced with larger contribution of S p-Cu d. This happens due to the shifting of delocalized S p-Cu d band position with respect to Cr t_{2g} level position, causing enhanced hybridization effect. The total energy calculations as shown in Fig. 1 and the related quantities tabulated in Table I suggest that this helps in stabilization of the FM phase, which, in turn, lends further support to the proposed kinetic-energy driven mechanism.

Substitution of S $3p$ by Se $4p$ anion causes expansion of the lattice by about 5%.[12] More delocalized Se $4p$ orbital is expected to hybridize stronger with Cr d states compared to S $3p$ orbital which, however, gets overcompensated by bond length enhancement, leading to slight shrinkage of the total bandwidth while the essential features remain the same as that of the S-based compound. Application of NMTO downfolding technique to estimate the renormalized on-site splitting at Se site, obtained by defining a few-band Se p only Hamiltonian, gives a value of about 4.1 eV. Our computed J (5.8 meV) and the mean-field T_c (505 K) show enhancement of T_c by 40 K, compared to that of the $CuCr_2S_4$ (see Table I), in good agreement with experimental enhancement of 53 K.[5]

To conclude, our analysis of the computed electronic structure of $CuCr_2X_4$ (X=S, Se) shows that the underlying exchange mechanism in these materials is the kinetic-energy driven mechanism as operative in the case of double perovskites or pyrochlores but with a twist.

As a passing comment, our model calculation with ∠Cr-S-Cr enhanced to 101° from the original value of 94.66° makes the compound nearly half-metallic with vanishing DOS in the minority spin channel, with the possibility that small disorder can completely suppress minority spin conduction. The computed mean-field T_c with nearest neighbor J turns out to be about more than twice as large as the original compound. For technological importance, it may be interesting to dope $CuCr_2S_4$ with some nonmagnetic element which can enhance the ∠Cr-S-Cr without changing the Cr-S bond length a lot.

The research was funded by DST Project No. SR/S2/CMP-42/2003. TSD thanks DST (Swarnajayanti) and DDS thanks CSIR (J.C. Bose) for assistance. MDR thanks DST (WOS-A).

[1] E. J. W. Verwey and P. Haayman, Physica (Amsterdam) **8**, 979 (1941).

[2] A. P. Ramirez, R. J. Cava and J. Krajewski, Nature (London) **386**, 156 (1997).

[3] M. D. Kaplan and B. G. Vekhter, *Cooperative Phenomena in Jahn-Teller Crystals* (Plenum Press, New York, 1995).

[4] H. M. Palmer and C. Greaves, J. Mater. Chem. **9**, 637 (1999).

[5] I. Nacatani, H. Nose, and K. Masumoto, J. Phys. Chem. Solids **39**, 743 (1978).

[6] V. N. Antonov, V. P. Antropov, B. N. Harmon, A. N. Yaresko, and A. Ya. Perlov, Phys. Rev. B **59**, 14552 (1999).

[7] Von Harry Hahn, C. de Lorent, and B. Harder, Z. Anorg. Allg. Chem. **283**, 138 (1956).

[8] F. Lotgering, in *Proceedings of the International Conference on Magnetism, Nottingham* (IOP, Bristol, 1964), p. 539.

[9] C. Colominas, Phys. Rev. **153**, 558 (1966).

[10] J. B. Goodenough, J. Phys. Chem. Solids **30**, 261 (1969).

[11] A. Kimura, J. Matsuno, J. Okabayashi, A. Fujimori, T. Shishidou, E. Kulatov, and T. Kanomata, Phys. Rev. B **63**, 224420 (2001).

[12] P. Villars and L. D. Calvert, *Pearson's Handbook of Crystallographic Data for Intermetallic Phases* (ASM International, Materials Park, OH, 1991).

[13] J. B. Goodenough, Phys. Rev. **100**, 564 (1955); J. Kanamori, J. Phys. Chem. Solids **10**, 87 (1959).

[14] Changing only the internal parameter u, associated with anion position, causes the change of the Cr-S bond length as well. The

lattice constants are therefore suitably adjusted so as to change only ∠Cr-S-Cr, keeping the Cr-S bond length fixed at the original value.

[15] O. K. Andersen and O. Jepsen, Phys. Rev. Lett. **53**, 2571 (1984).

[16] We have checked the validity of our calculations in terms of the full-potential LAPW (P. Blaha, K. Schwartz, G. K. H. Madsen, D. Kvasnicka, and J. Luitz, WIEN2K) calculation as well.

[17] We note that the spin polarization at the Cu site is small compared to that at S sites in the unit cell, indicating that the antiparallel moment is primarily contributed by S.

[18] D. D. Sarma, P. Mahadevan, T. Saha-Dasgupta, S. Ray, and A. Kumar, Phys. Rev. Lett. **85**, 2549 (2000); D. D. Sarma, Curr. Opin. Solid State Mater. Sci. **5**, 261 (2001).

[19] T. Saha-Dasgupta and D. D. Sarma, Phys. Rev. B **64**, 064408 (2001).

[20] A. Läuchli, F. Mila, and K. Penc, Phys. Rev. Lett. **97**, 087205 (2006); T. Saha-Dasgupta, M. De Raychaudhury, and D. D. Sarma, Phys. Rev. Lett. **96**, 087205 (2006).

[21] D. D. Sarma, W. Speier, R. Zeller, E. van Leuken, R. A. de Groot, and J. C. Fuggle, J. Phys.: Condens. Matter **1**, 9131 (1989).

[22] O. K. Andersen and T. Saha-Dasgupta, Phys. Rev. B **62**, R16219 (2000).